WATER RESOURCES RESEARCH, VOL. 33, NO. 8, PAGES 1983–1991, AUGUST 1997

Experimental evidence of dynamic scaling and indications of self-organized criticality in braided rivers

Victor B. Sapozhnikov and Efi Foufoula-Georgiou

Saint Anthony Falls Laboratory, University of Minnesota, Minneapolis

Abstract. The evolution of an experimental braided river produced in our laboratory has been monitored and analyzed. It has been shown that in addition to the spatial scaling revealed by *Sapozhnikov and Foufoula-Georgiou* [1996a], braided rivers also exhibit dynamic scaling. This implies that a smaller part of a braided river evolves identically (in the statistical sense) to a larger one provided the time is renormalized by a factor depending only on the ratio of the spatial scales of those parts. The small value of the estimated dynamic exponent z is interpreted as an indication that the evolution of small channels in a braided river system is to a large extent forced by the evolution of bigger channels. The presence of dynamic scaling is further interpreted as indicating that braided rivers may be in a critical state and behave as self-organized critical systems.

1. Introduction

In a recent paper [*Sapozhnikov and Foufoula-Georgiou*, 1996a] evidence was presented that natural braided rivers exhibit anisotropic scaling (self-affinity) in their geometrical structure, within a range of scales spanning the width of the narrowest channel to the width of the braid plain. In simple words, within these scales, if a small part of a braided river is stretched in a certain way along the mainstream direction and a certain different way along the perpendicular direction, then this stretched part looks statistically the same as a bigger part of the river. Such anisotropically scaled objects are called self-affine fractals and are characterized by two fractal exponents ν_x and ν_y. The ratio ν_x/ν_y characterizes the scaling anisotropy, and the fractal dimension $D = (\nu_y - \nu_x + 1)/\nu_y$ [e.g., see *Sapozhnikov and Foufoula-Georgiou*, 1995] indicates how densely the object fills the space.

In *Sapozhnikov and Foufoula-Georgiou* [1996a], three natural braided rivers of different scales and different hydrological and sedimentological characteristics (Aichilik and Hulahula in Alaska and Brahmaputra in Bangladesh) were analyzed for spatial scaling using the logarithmic correlation integral (LCI) method developed by *Sapozhnikov and Foufoula-Georgiou* [1995]. Interestingly enough, it was observed that despite their different scales (0.5–15 km in braid plain width), slopes (7×10^{-3}–8×10^{-5}), and types of bed material (gravel to sand), all three rivers exhibited anisotropic spatial scaling with almost the same fractal exponents: $\nu_x = 0.72$–0.74 and $\nu_y = 0.51$–0.52, the x axis being oriented along the river and the y axis being in the perpendicular direction. In simple terms this implies that if parts of a braided river are stretched by λ along the mainstream direction and by $\lambda^{\nu_y/\nu_x} \simeq \lambda^{0.7}$ along the perpendicular direction, the resulting images will look statistically similar to each other (similarity within a braided river). At the same time the invariance of ν_x and ν_y between braided rivers of different sizes and hydrology/sedimentology suggests that the same anisotropic scaling as above applied to different rivers will result in statistically similar images, apart, possibly, from a normalization factor to account for the different mass of each river. (Note that "mass" here refers to the area, i.e., number of pixels, covered with water.) The presence of such a statistical scale invariance in the spatial structure of braided rivers, apart from being interesting in its own right, might indicate the presence of universal features in the underlying mechanisms responsible for the formation of braided rivers and deserves further theoretical and experimental investigation.

Braided rivers, besides their complex geometry at any instant of time, are also highly dynamic systems characterized by intensive erosion, sediment transport and deposition, and frequent channel shifting as they evolve. Predicting the evolution of braided rivers in terms of frequency and magnitude of channel shifting is of paramount importance where hydraulic structures or land developments are planned or where field use must be made of maps and air photos. It is of great practical and theoretical value therefore to study the evolution of braided rivers in addition to their spatial structure. In view of the evidence for spatial (static) scaling in braided rivers the question is asked here as to whether they also show dynamic scaling. The presence of dynamic scaling would imply that space and time can be appropriately rescaled such that the evolution of the spatial structure of parts of the river of different size would be statistically indistinguishable. The presence of dynamic scaling would also provide a highly desirable integrated framework for studying, simultaneously, the spatial and temporal structure of braided rivers.

2. Dynamic Scaling: A Theoretical Framework

The idea of dynamic scaling can be qualitatively presented as follows. Suppose there is a fractal object, of fractal dimension D, which evolves in time such that its fractality is preserved at all times. In our case the fractal object is the spatial pattern of the active channels constituting a braided river which was shown to exhibit spatial scaling by *Sapozhnikov and Foufoula-Georgiou* [1996a]. The fractality (spatial scaling) of the object implies that if one takes a picture of a part of the object of size $L_1 \times L_1$ and a picture of a larger part of the same object of size $L_2 \times L_2$ and projects these two pictures onto two screens of the same size, the images on the screens will be statistically

Paper number 97WR01233.
0043-1397/97/97WR-01233$09.00

indistinguishable. Suppose now that one makes another step and, instead of taking still pictures, videotapes the two regions and observes the evolution of the images on the two screens. In contrast to the still pictures the movies will not be statistically indistinguishable. The rate of the evolution will be different (slower for the larger scale). If, however, there exists a dynamic exponent z such that for every L_1 and L_2 it is possible to rescale the time as

$$\frac{t_2}{t_1} = \left(\frac{L_2}{L_1}\right)^z \tag{1}$$

or, in other words, to play the movies at different speeds such that the rate of the evolution is the same on both screens, then we say that in addition to static (spatial) scaling, the system also shows dynamic scaling.

Let us characterize the evolution of a stationary fractal object by "changes" in its pattern, where changes are defined as parts of the space which were not occupied by the object at a certain moment of time but became occupied after some time lag t. Let $n(L, l' > l, t)$ denote the number of changes exceeding size l after some time lag t in a region of size $L \times L$. By definition, changes can only occur in parts of the space occupied by the object. In other words, changes follow the pattern of active channels, and thus, at every scale they are not present in those parts of the space where active channels are not present. Because the object is fractal, with a fractal dimension D, the number of changes scales with the size of the observed region (see appendix) as

$$n(L_2, l' > l, t) = n(L_1, l' > l, t)\left(\frac{L_2}{L_1}\right)^D \tag{2}$$

The presence of dynamic scaling, implying the same rate of evolution after rescaling (equation (1)) is applied, means that the number of changes exceeding sizes l_1 and l_2 after time lags t_1 and t_2 in the regions of size $L_1 \times L_1$ and $L_2 \times L_2$, respectively, is the same on both screens, i.e.,

$$n(L_1, l' > l_1, t_1) = n(L_2, l' > l_2, t_2) \tag{3}$$

provided that the changes are of the same relative size, i.e.,

$$\frac{l_1}{L_1} = \frac{l_2}{L_2} \tag{4}$$

and time and space have been rescaled such that

$$\frac{t_1}{L_1^z} = \frac{t_2}{L_2^z} \tag{5}$$

We stress here that L_1 and L_2 are not the sizes of two different systems but sizes of two different regions of the same system.

Suppose now that we fix the scale of the region of interest to L_2 and that instead of zooming to different scales, we follow the distribution of changes in this region as the object evolves. From (2) and (3) we obtain for the distribution of changes in the region $L_2 \times L_2$

$$n(L_2, l' > l_1, t_1)\left(\frac{L_1}{L_2}\right)^D = n(L_2, l' > l_2, t_2) \tag{6}$$

which is true provided (4) and (5) hold. The variable L_2 is the same in both sides of (6) and therefore can now be dropped. Replacing L_1/L_2 by l_1/l_2 (because of relation (4)) yields

$$l_1^D n(l' > l_1, t_1) = l_2^D n(l' > l_2, t_2) \tag{7}$$

Finally, we obtain the condition for the distribution of changes in a system showing dynamic scaling: there exists a dynamic exponent z such that if (5) is true, i.e., $t/L^z = \text{const}$ (which according to (4) also implies $t/l^z = \text{const}$), then $l^D n(l' > l, t) = \text{const}$, or, in other words, the distribution of changes in such systems can be expressed as

$$n(l' > l, t) = l^{-D} f\left(\frac{t}{l^z}\right) \tag{8}$$

where $f(\quad)$ is some function.

To understand the form of that distribution, let us now consider the asymptotic properties of the function $f(t/l^z)$. This function has to level off at big values of the argument t/l^z. Indeed, for big enough time lags, such that the object decorrelates completely between two snapshots, the difference between the two patterns of the object (and therefore the distribution of changes $n(l' > l, t)$) does not depend on time anymore. This implies that $f(t/l^z) = \text{const}$, and, consequently, that $n(l' > l, t) = \text{const} \times l^{-D}$, for big enough values of t/l^z. For time lag $t = 0$, there are no changes in the object, which implies that $n(l' > l, 0) = 0$ and, correspondingly, that $f(0) = 0$. If for small values of the argument the function f can be approximated by a power law, with some exponent β, then the condition (8) for dynamic scaling takes the form

$$n(l' > l, t) \sim t^\beta l^{-D-\beta z} \tag{9}$$

It is noted here that the theoretical framework for the description of dynamic scaling of stationary fractal objects as developed above differs from the existing frameworks for dynamic scaling of nonstationary growing objects which has been extensively investigated in the past. For example, dynamic scaling of simulated growing interfaces has been studied by *Edwards and Wilkinson* [1982], *Family* [1986], *Meakin et al.* [1986], *Kardar et al.* [1986], and others [see also *Family and Vicsek*, 1991; *Vicsek*, 1992]. Recently *Czirok et al.* [1993] demonstrated experimentally dynamic scaling in a micromodel of landscape evolution. In these studies the evolution of a fractal surface is described by two exponents α and β corresponding to the spatial and temporal scaling of the surface roughness. In particular, the width or the standard deviation $w(L, t)$ of a surface of linear extent L scales as L^α for long times and as t^β at the early stages of the process. According to the corresponding dynamic scaling theory, the width follows a double-scaling equation $w(L, t) \sim L^\alpha f(t/L^{\alpha/\beta})$ where $f(\quad)$ is some function. (The fractal dimension of the rough surface D relates to α as $D = d - \alpha$, where d is the embedding dimension.)

As one can see, the theoretical framework for dynamic scaling of nonstationary growing objects is based on the analysis of the systematic change of a "macroscopic" parameter (width of the surface in the case described above) which essentially describes, in a statistical sense, the nonstationarity of such objects. Obviously, such an approach is not applicable to stationary objects where macroscopic parameters do not change systematically (although they can fluctuate around some average value). Therefore, in the theoretical framework of dynamic scaling of stationary fractal objects developed here we introduced the concept of changes in an evolving stationary object and expressed its dynamic scaling in terms of space-time scale invariance of the probability distribution of these changes. It is believed that the developed framework will be useful for the study of dynamic scaling in natural objects that could not be studied so far under the existing frameworks.

3. Experimental Study of Braided Rivers

One of the reasons that field workers have primarily focused on the detailed study of flow and sediment flux in small areas of braided rivers is the logistical difficulty of studying a complex, continually evolving river system over a large area. The fundamental problems in obtaining data sets characterizing the statistical properties of braided rivers are the high degree of variability in local quantities such as flow depth or sediment flux and the rapidity with which these change with time if the system is active. Thus field data from in situ measurement are difficult to find. Field data can, however, be obtained relatively easily (although tediously) on the static planform morphology of natural braided rivers by determining the presence or absence of water from an air photo or satellite image. For example, the data for the three braided rivers used in the study by *Sapozhnikov and Foufoula-Georgiou* [1996a] were obtained by the tracing of air photos and the digitization of the traced images. Even then, however, care must be taken to insure that data are taken from river sections in which downstream changes in discharge, grain size, vegetation, etc., are minimal so that each reach may be taken as statistically stationary. In the near future it is hoped that improved satellite technology will offer the means of obtaining accurate and frequent monitoring of the spatially and temporally variable flow distribution of natural braided river systems [e.g., see *Smith et al*., 1995, 1996]. To allow study of the detailed structure of braided rivers, higher resolution satellite images than those available today and wider coverage of areas of interest are needed.

Laboratory models of braided rivers can offer an excellent means of advancing our understanding of the complex dynamics of braided rivers. They offer an environment which permits us to control the physical parameters governing the evolution of the river and to obtain high-resolution images (e.g., see *Schumm et al*. [1987] for an interesting discussion of the advantages of using laboratory experiments in addition to monitoring natural rivers). Braiding is relatively easy to reproduce in the laboratory, and previous studies [*Ashmore*, 1991; *Kuhnle*, 1981; *Leddy et al*., 1993; *Schumm and Khan*, 1972] have shown that laboratory-scale streams exhibit qualitative features and behavior similar to natural rivers. Quantitative similarity can also be attained but only for gravel bed prototypes [*Ashmore*, 1982, 1985]. Given our emphasis on global statistical properties of braided rivers, both at one instant and as a function of time, experiments provide a useful way of obtaining additional data that can help us to understand the dynamics of braided rivers. The Saint Anthony Falls Laboratory at the University of Minnesota offers an ideal setting for such experiments. In fact, it houses the recently established Experimental Facility for the Study of Large Scale River Morphology and Landscape Evolution funded by NSF's Academic Research Infrastructure Program.

The size of our experimental basin is 5 m $\times$ 0.75 m. Sediment and water were supplied continuously at a precisely controlled rate using a constant rate AccuRate auger feeder and a constant height water tank. The sediment and the water were combined together in a mixing funnel before injection into the basin. The grain size of the supplied sediment was 0.12 ± 0.03 mm. The water discharge was 20 g s^{-1}, and sediment supply was 0.6 g s^{-1}. The river was left to evolve until its slope (calculated from the bed elevations measured by point gauge) stabilized at the value of 0.15, which happened 8 days after the initiation of the experiment. The same sediment was used throughout the experiment (i.e., while building up the slope and afterward). The walls of the experimental basin were covered with rough rubber material to reduce the attraction of channels to the walls. To minimize the boundary effects, the data on the river evolution were collected in periods when the river did not touch the walls. Video camera and still cameras recorded the evolution of the system. To visualize the river and monitor its depth, dye was supplied continuously during each videotaping session. For that the sediment supply was switched to another AccuRate auger feeder where the sediment was mixed with the dye powder. This provided the same sediment supply rate as the first feeder, within an accuracy of 5%. After each videotaping session the dye was left to be flushed out of the system and the basin was dye-free in a few hours. We started collecting data 6 days after the slope stabilized, and three videotapes, each covering approximately 40 min of the river evolution in different days, were collected. The studied region was 0.75 m $\times$ 1.0 m, starting 3 m downstream from the injection point. The recording time of an image was 1/60 s. The video camera produced images of 240 lines with 1125 points in each line. The recorded data were then digitized for treatment and analysis. The digitized images had 480 $\times$ 640 pixels. Therefore the resultant digitized images resolved 240 pixels across the river and 640 pixels along the river. For the studied region size (0.75 m $\times$ 1.0 m) this implies a resolution of 3 mm across the river and 1.5 mm along the river. The vertical distance between the camera and the river was 3.1 m. A different angle of observation of the central part and lateral parts of the basin distorts the image (the image of an object in a lateral part of the basin is smaller than the image of an object of the same size in the central part). We measured this distortion and found that it was approximately 2%. The experimental rivers showed a high degree of braiding (e.g., see Figure 1) and active dynamics. Significant changes were recorded in periods of less than 1 min. Here we present the results of analysis of the river evolution recorded in one of the videotapes with the best quality of the image. Similar results were obtained from the analysis of the other two videotapes.

Extracting the river patterns for statistical analysis presented significant difficulties because very soon the sediment was colored with the same dye as the water. However, extracting changes in the river patterns by subtracting images taken at different moments of time proved feasible and quite robust. These changes (depicted as differences in the darkness of the images) are the result of water depth increase or decrease which includes the cases of covering with water a previously dry area or exposing a previously covered area. We used these changes to characterize the evolution of the braided river following the approach developed in section 2. For short enough time lags (such that the colored sediment patterns are almost the same and get zeroed when subtracted) the differences in the two images represent only true changes in the active channel patterns. However, the time lag cannot be made too short (less then approximately 3 s) because in that case the difference between two pictures of the river is small and becomes comparable to the noise introduced by the video camera. At the same time we could not use long time lags (more than approximately 1 min) because in these time lags the patterns of the colored sediment change significantly and subtracting the two images creates spurious (i.e., not caused by the river pattern evolution) changes which erroneously contribute to the probability distribution of changes.

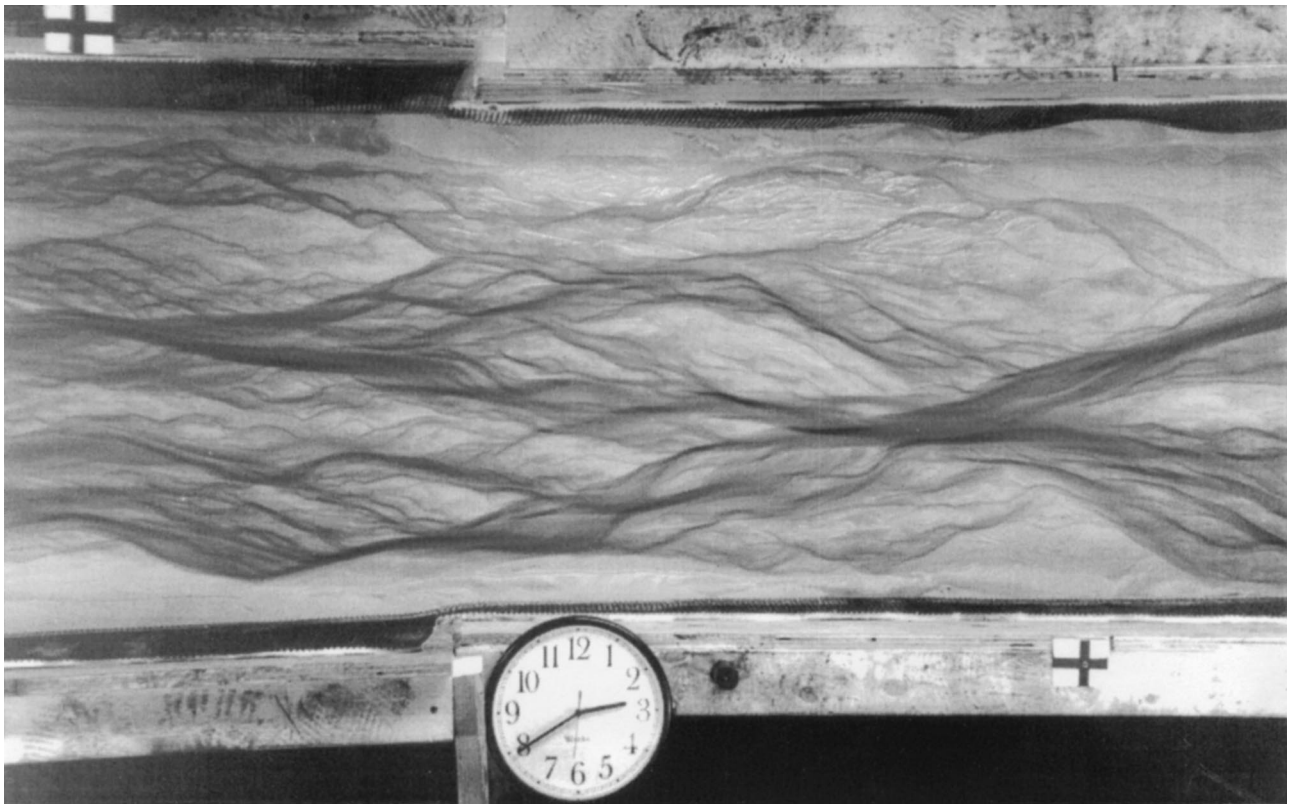

Figure 1. A braided river produced in our laboratory. Channels are indicated by dark areas.

4. Dynamic Scaling in the Experimental Braided River

To study scale relationships in the evolution of braided rivers and test the presence of dynamic scaling, we monitored the changes in our experimental braided river as it evolved and did a statistical analysis of these changes. By monitoring the evolution of the river, we collected 90 frames with a time step of 1 s. The collected patterns were digitized, and, by subtracting these patterns from each other, changes in the braided river were obtained for different time lags (3 s to 1 min). For example, Figure 2a shows a picture of a part of the experimental braided river, and Figure 2b shows the same region 15 s later. Figure 2c displays parts of the basin that were covered with water in Figure 2a but became shallower or exposed in Figure 2b 15 s later ("old" changes). Figure 2d shows parts of the basin that were shallower or not covered with water at all in Figure 2a but became deeper or covered in Figure 2b ("new" changes). Thus, although changes in a river are three-dimensional structures, as is the river itself, in this study we only consider their projections onto a horizontal plane (i.e., when we say "sizes of changes in the river" we imply sizes of their projections). We then apply to the projections the theoretical framework developed in section 2 for two-dimensional objects. In doing that, changes (i.e., parts of the space whose occupancy status switched after some time) are treated equally no matter whether they were located at the elevation of the river bed (e.g., when water conquered dry areas) or higher (e.g., when water level rose in some area). See also section 7 for further discussion of this issue.

It should be noted that dye does not go away immediately from the regions left by active channels, which complicates the observation. Therefore, for quantitative analysis we chose "new" changes (shown in Figure 2d) and not "old" changes (Figure 2c). We made sure (by direct observation of chosen areas) that when colored water conquered a dry area, the area became darker even if its sediment was already colored so we did not miss the new changes. We kept the periods of dye influx short to prevent the sediment from becoming too dark. To eliminate the noise introduced by the video camera, the pixels where the difference between the two subtracted images was very small (less than 24 out of 256 degrees of brightness) were zeroed. Then the cumulative probability distributions of the sizes of changes (characterized by the square root of their areas) were estimated. The distribution of changes was followed over time, and Figure 3 shows these distributions for time lags of 3, 4, 5, 7, 9, and 15 s. Notice that the number of changes of size greater than l in a time lag t, $n(l' > l, t)$, is plotted instead of the probability. As can be seen from Figure 3, these distributions can be well approximated by power laws for different time lags, and the slopes of the log-log plots of the distributions found for different time lags are very close, so they can be viewed as being related by a parallel shift in the log-log scale. In other words, the distributions can be presented in the form

$$n(l' > l, t) = g(t)l^{-k} \tag{10}$$

where $n(l' > l, t)$ is the number of new changes (Figure 2d) of size greater than l for time lag t and $g(t)$ is a function of time lag t.

The log-log plot of $n(l' > l, t)l^k$ against t shown in Figure 4 suggests that for small values of t, $g(t)$ shows a power law dependence

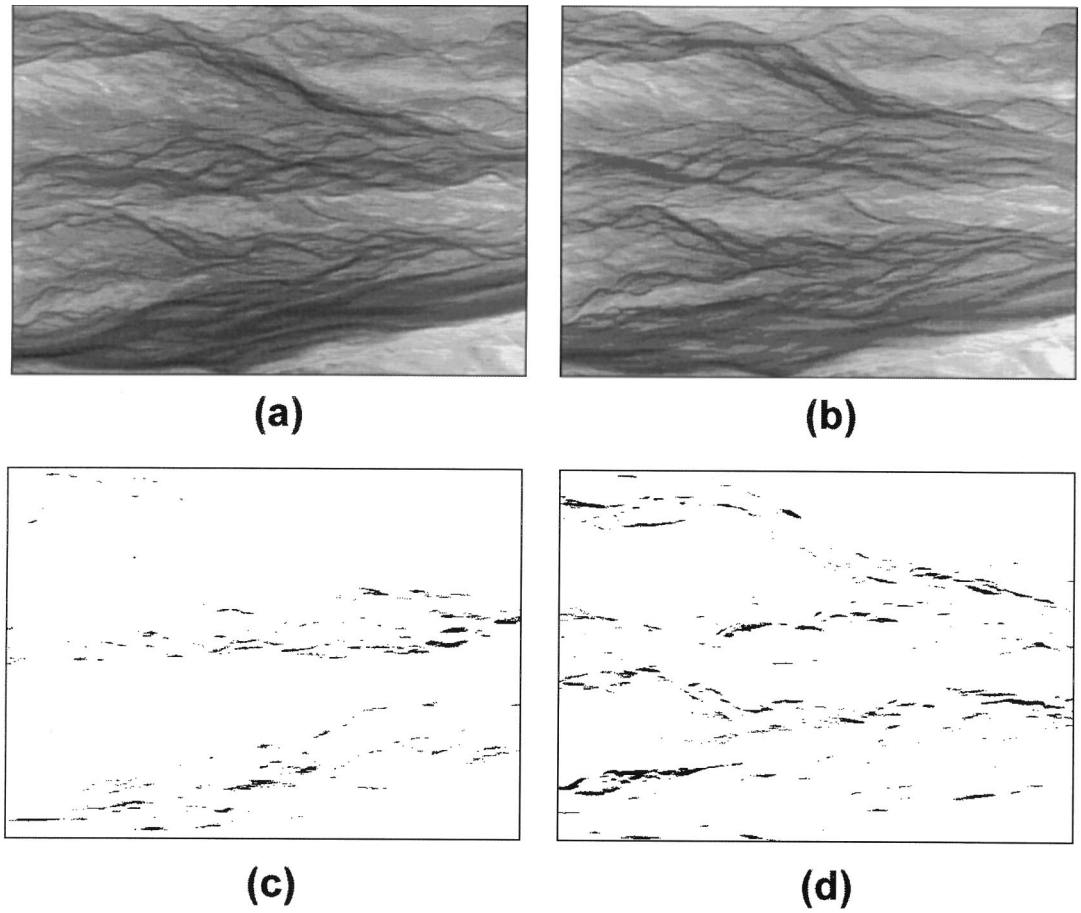

Figure 2. (a) Image of a part of the experimental braided river; (b) the same region 15 s later; (c) parts of the basin that were covered with water in Figure 2a but became shallower or exposed in 15 s (old changes); (d) parts of the basin that were shallower or not covered with water at all in Figure 2a but became deeper or covered in Figure 2b (new changes).

$$g(t) \sim t^{\beta} \tag{11}$$

Equations (10) and (11) can be combined in one equation showing the temporal evolution of the distribution of changes

$$n(l' > l, t) \sim t^{\beta} l^{-k} \tag{12}$$

It is easy to see that this equation coincides with (9) expressing dynamic scaling (for small values of t/l^z) with the dynamic exponent z given as

$$z = (k - D)/\beta \tag{13}$$

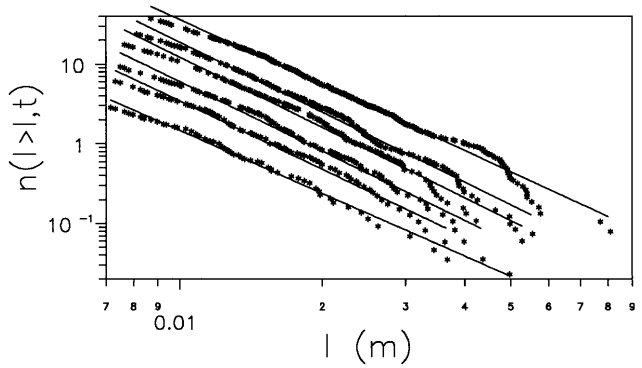

Figure 3. Number of solid areas in Figure 2d (new changes), $n(l' > l, t)$) of size greater than l for time lags t of 3, 4, 5, 7, 9, and 15 s (from bottom to top). The sizes of changes are measured as the square root of their areas. The plot suggests that the distributions have broad central regions that are well approximated by power laws, and their slopes for different time lags are very close.

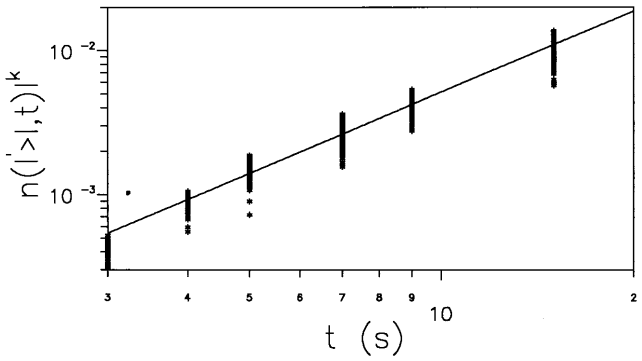

Figure 4. Evolution of the distribution of changes shown by the time dependence of the function $n(l' > l, t)l^k$. The plot suggests that power law dependence applies well over a major part of the range.

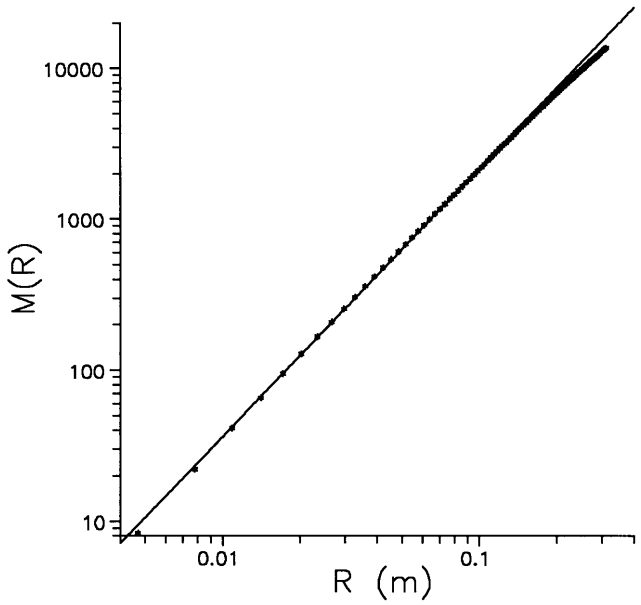

Figure 5. Spatial scaling in the experimental braided river indicated by straight line log-log dependence of its mass M (the number of pixels covered with water) within a square box versus the size of box R. The estimated value of D is 1.75.

Equations (1) and (8), in general, and (1), (12), and (13), in particular (the power law dependence (equation (12)) being suggested by the braided river data for small values of t/l^z), integrate spatial and temporal scaling characteristics under the unifying framework of dynamic scaling.

In principle, the parameter z (dynamic exponent) can be estimated directly from (8). That is, by nonlinear optimization the value of z that minimizes the spread of the points $n(l' > l, t)l^D$ versus t/l^z (so that all curves collapse to a single curve f) can be found. However, we preferred to take advantage of the power law dependence (equation (12)) suggested by the data and to follow a stepwise estimation approach. Namely, we use the power law distribution of changes (Figure 3 and equation (10)) to estimate k and the power law dependence of $g(t)$ (Figure 4 and equation (11)) to estimate β. Then z is estimated from (13). Specifically, from the slopes of the plots shown in Figures 3 and 4 the exponent k in (10) was estimated as 2.8 and the exponent β in (11) was estimated as 2.0. The fractal dimension of the experimental braided river D was estimated from one pattern of the river by the "mass-in-a-box" method [e.g., see *Mandelbrot*, 1982] as 1.75 (see Figure 5). These estimates gave an estimate of the dynamic scaling exponent from (13) as $z \simeq 0.5$.

It is important to note that although for small time lags Figure 3 shows reasonably good temporal scaling, it deviates from the power law behavior for bigger time lags. It should be stressed, however, that this does not indicate the loss of dynamic scaling (expressed by the general equation for dynamic scaling (8)). Indeed, as discussed in section 2, even if the function f, from (8), follows a power law at small values of the argument, it has to level off at big values of the argument which necessarily leads to the loss of power law dependence in relation (11) but not to the loss of dynamic scaling. In fact, to confirm that the distributions corresponding to different time lags satisfy the general equation for dynamic scaling (8), we plotted for $z = 0.5$ the values of $n(l' > l, t)l^D$ versus t/l^z for different time lags up to 1 min in Figure 6. As one can see, all curves satisfactorily collapse to a single curve (the $f(t/l^z)$ function). This further corroborates the presence of dynamic scaling and the adequacy of the estimated dynamic exponent $z \simeq 0.5$ in the experimental braided river. Notice that this last confirmation of dynamic scaling, i.e., that the general equation for dynamic scaling (equation (8)) holds, did not directly use the assumption of power law distribution of changes (equation (10)) or power law dependence of $g(t)$ for small values of t (equation (11)). These two special forms of dependencies (suggested directly from the experimental data in Figures 3 and 4) were conveniently used only to estimate z in a stepwise manner via (13). After the value of z was estimated, plotting $n(l' > l, t)l^D$ versus t/l^z and seeing that all curves collapse to a single curve provides additional and independent evidence of dynamic scaling.

We would like to point out that on the basis of the study of *Sapozhnikov and Foufoula-Georgiou* [1996a], the experimental braided river is expected to be a self-affine object (characterized by two scaling exponents ν_x and ν_y) and not a self-similar object (characterized by a single fractal dimension D). Despite this, the above developments of dynamic scaling were presented in terms of a single fractal dimension D. This is because, as discussed also later in section 7, extension of the dynamic scaling theory to self-affine objects has not yet been achieved and should form the focus of further research. Moreover, it is noted that even if that theory were available at present, our experimental data did not even permit an estimation of ν_x and ν_y for two main reasons: (1) the river segment was too short to get an accurate estimate via the LCI method, and (2) it was hard to separate the river from the colored sediment in the video images in order to produce reliable tracings of the river pattern. Note that this was not a problem for changes in the river pattern because the colored sediment was zeroed by subtraction. Despite the above limitations, we note that the presented dynamic scaling developments are still valid for a self-affine object, and D can be seen as a surrogate parameter for D_G (global fractal dimension) of the braided river which relates to ν_x and ν_y via the expression given by *Sapozhnikov and Foufoula-Georgiou* [1995]: $D_G = (\nu_y - \nu_x + 1)/\nu_y$. Of course, further refinement of the developed framework to self-affine objects characterized by ν_x and ν_y is desirable, but this is an issue for further study.

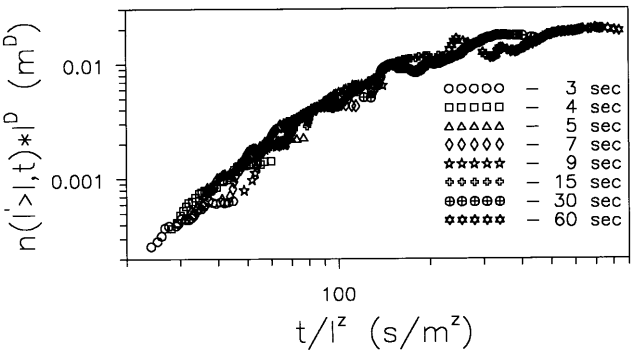

Figure 6. Plot showing that the rescaled distributions of changes collapse into a single curve (equation (8)). Time lags from 3 to 60 s (bottom left to top right) are shown. This further corroborates the presence of dynamic scaling and the adequacy of the estimated value of the dynamic exponent as $z \simeq 0.5$ for the experimental braided river.

5. Physical Interpretation of Dynamic Scaling

In any natural phenomenon, large-scale statistical symmetries or scale invariances, if found present, are believed and hoped to be related to the physical mechanisms that created the space-time structure of the process at hand, although establishing and understanding these relations very often turns out to be a nontrivial task. So what does the value of the dynamic exponent indicate for the physical mechanisms of a braided river? First, on the basis of (1) the estimated value of the dynamic exponent $z \simeq 0.5$ implies that if one increases the spatial scale by, say, 10 times, the evolution of the system slows down by $10^{0.5} \simeq 3$ times. In other words, for instance, it implies that the lifetime of the channels in a braided river system scales with channel size such that 10 times smaller channels disappear approximately 3 times faster. Furthermore, the low value of the dynamic exponent $z \simeq 0.5 \ll 2$ indicates a relatively weak dependence of the rate of evolution on the spatial scale. This provides insight into the physical processes governing the evolution of braided rivers. Indeed, this value of z is significantly lower than the typical values of the dynamic exponent, which are usually 2 or higher [e.g., see *Ma*, 1976]. For example, as a simple case, if the lifetime of a channel were controlled by a diffusion-type process, it would be proportional to the square of the scale, which would imply that $z = 2$. On the other hand, if we hypothetically imagine as a limiting case that the small channels do not evolve by themselves at all and only appear or disappear because (and when) the bigger channels feeding them appear or disappear, then the lifetime of smaller and bigger channels would be the same, which would mean that no temporal rescaling is required when going from one spatial scale to another. This would imply that $z = 0$. Thus the small value of z obtained for braided rivers indicates strong correlation between the evolution of large and small channels within a braided river system. This leads to the conjecture that the evolution of small channel patterns is to a great extent forced by the evolution of larger channels. Notice that further support for this conjecture is provided by the fact that the other way around, i.e., changes in small channels forcing changes in large channels, would require a spontaneous synchronization in evolution of small channels which feed a larger one, and this does not seem feasible. Indeed, for a larger channel to disappear as a result of the disappearance of the smaller channels feeding it, smaller channels would have to disappear at the same time. At this point we do not see a mechanism for such a synchronization.

6. Are Braided Rivers Self-Organized Critical Systems?

The self-organized criticality (SOC) concept introduced by *Bak et al*. [1987] states that many nonlinear systems with extended degrees of freedom self-organize into a critical state in a natural way, i.e., without any tuning parameter (e.g., temperature) which is needed to bring traditional equilibrium systems to a critical state [see, e.g., *Ma*, 1976; *Patashinskii and Pokrovskii*, 1979]. The concept of SOC has been found useful in many scientific and engineering applications, for example, earthquake prediction, snow avalanche prediction, description of solar flares, description of forest fires, etc. [see *Bak and Paczuski*, 1993]. In the past few years the SOC concept has been explored for drainage network landscape evolution [e.g., *Takayasu and Inaoka*, 1992; *Rinaldo et al*., 1993] and, recently, has been claimed by *Stølum* [1996] for dynamics in the fluid mechanical model of a meandering river developed by G. Parker, A. E. Howard and coworkers [e.g., see *Parker and Andrews*, 1986; *Howard and Knutson*, 1984].

In a recent publication, *Sapozhnikov and Foufoula-Georgiou* [1996b] have questioned the applicability of the SOC concept to models of erosional landscape evolution. They have argued that none of the states of these modeled landscapes can be considered critical and that the resulting landscapes show scaling in space characterized by fractal geometry but not scaling in time as they do not allow any changes under perturbations let alone "catastrophic" changes possible for a system in a critical state. However, we believe that braided rivers are systems where the SOC concept naturally applies. Braided rivers (1) are nonlinear systems, (2) obviously have an enormous number of degrees of freedom, (3) show collective behavior which is a crucial feature of systems in a critical state, (4) exhibit spatial scaling [see *Sapozhnikov and Foufoula-Georgiou*, 1996a], and (5) undergo significant changes over a wide range of scales even when they are statistically in equilibrium. Moreover, evidence was presented in this study for the presence of dynamic scaling as well, which is an important characteristic of systems at the critical state. It should be noted that the experimental braided river system brought itself to the state at which it showed dynamic scaling by just being uniformly supplied with water and sediment, i.e., without tuning any physical parameter of the experimental model. It happened in the same way as in the sandpile model [*Bak*, 1987], where the system builds up itself without any tuning and shows spatial and temporal scaling. For all of the above reasons we conjecture that braided rivers may be self-organized critical systems.

Studying braided river dynamics under the SOC framework offers the potential of using the apparatus of the theory of critical state which provides a general framework for description and understanding of all critical phenomena and enables one to apply results obtained for known systems (e.g., magnetic fields and percolation clusters) to new systems less well known. An example of this idea is presented by *Tang and Bak* [1988]. Strictly speaking, to firmly establish SOC, one would also need to follow the behavior of the braided river as it approaches the critical state (perhaps with the critical slope playing the role of critical temperature here). Such experiments, however, are very hard to perform (even in other more controlled physical systems), and thus spatial and dynamic scaling of the type presented here is usually considered adequate evidence for SOC. Nevertheless, more data analysis of the braided river before, as it approaches stationarity, and after its slope stabilizes, is needed to firmly establish whether and under what conditions braided rivers can be considered self-organized critical systems.

7. Conclusions and Open Problems

In a previous study, *Sapozhnikov and Foufoula-Georgiou* [1996a] presented evidence that braided rivers exhibit spatial (static) scaling in their morphology. In this study we presented evidence that braided rivers exhibit dynamic scaling too, which implies that it is possible to renormalize space and time such that a smaller part of a braided river evolves identically (in a statistical sense) to a larger part of the river. The presence of dynamic scaling is not only interesting in its own right but also promises to shed light upon the space-time dynamics of braided rivers by unraveling statistical similarities between pat-

terns at smaller space-time scales and those at larger space-time scales. The dynamic scaling relationships established here can also be used to statistically predict long-term changes of the system at a larger spatial scale on the basis of monitored short-term changes at a smaller spatial scale. The evidence for dynamic scaling was further interpreted as an indication that braided rivers may be in a critical state and behave as self-organized critical systems. From experimental braided river data produced in our laboratory the value of the dynamic exponent z for the space-time rescaling in (1) was established to be approximately equal to 0.5. This value of z was interpreted as an indication of a relatively weak dependence of the rate of evolution on the spatial scale in braided rivers. In particular, it lead us to conjecture that changes in small channel patterns are to a great extent forced by the changes in larger channels.

Our analysis presents a first attempt to study the large-scale dynamics of braided rivers and to seek spatiotemporal invariances in those systems. Of course, more theoretical, empirical, and experimental research is needed to fully study the space-time evolution of these complex systems and their scale relations. Some open problems follow.

In our analysis the evolution of the braided river system has been characterized by the horizontal sizes of changes. An interesting direction for further research is the introduction of the third dimension, i.e., consideration of the depth of changes in addition to their horizontal sizes. This approach would enable one to explore braided rivers for "dynamic multiscaling."

In our study we analyzed changes in the river by subtracting two images of the river taken at different moments of time. In doing that we did not distinguish between changes caused (1) by the flooding of previously dry areas of the basin and (2) by the increase of water depth in areas which were already covered with water. This separation was not feasible with our data because sediment coloring did not allow us to determine with certainty from the darkness of the image whether a particular location was or was not covered with water. A more detailed analysis which would include separation of these two cases may be of interest, but this would require a different technology than sediment coloring which would permit accurate determination of water depth (and not water depth change only) at every point of the basin. Such data would permit study of the space-time structure of water depth too and thus characterization of the hydrology in addition to the morphology of braided rivers.

Also, an important issue for future study should be the extension of the developed theoretical framework of dynamic scaling to self-affine objects. That is, if the underlying object is self-affine and is characterized by two fractal exponents ν_x and ν_y, expressions of dynamic scaling should be developed in terms of ν_x and ν_y (or in terms of the two fractal dimensions D_G and D_L) (see *Sapozhnikov and Foufoula-Georgiou* [1995, 1996a] for the connection of ν_x and ν_y to D_G and D_L). An associated open problem is the theoretical description of the critical state of self-affine objects. Such a theory does not exist to our knowledge, probably because there was no need for it in traditional (not self-organized) critical systems. Another important issue to be explored is the connection of dynamic scaling not only to the fractal geometry of braided rivers but also to other scaling characteristics of natural and simulated braided rivers, such as power law distributions in channel widths and bar sizes [e.g., see *Howard et al*., 1970; *Barzini and Ball*, 1993; *Murray and Paola*, 1994; *Sapozhnikov and Foufoula-Georgiou*, 1996a].

It should be stressed that our analysis applies to the comparison of small and large parts of one river system and not of one system with another. The latter would require inclusion of other physical parameters which govern the evolution of rivers. For example, slope plays a crucial role in the rate of the evolution of rivers (the greater the slope, the faster the evolution). For example, the slope of Brahmaputra is 2000 times lower than that of our experimental river, which significantly affects their relative rates of evolution. Other important factors are total water and sediment flux in a river (the greater the imposed flux, the faster the evolution) [*Ashmore*, 1985] and the type of the sediment. Thus, to relate the rate of the evolution of different systems, (1) has to be extended. Under a scaling hypothesis one could conjecture that it would take the form

$$\frac{t_2}{t_1} = \left(\frac{L_2}{L_1}\right)^z \left(\frac{s_2}{s_1}\right)^\gamma \cdots \tag{14}$$

where s is the slope of a river and the dots imply that other parameters could enter this equation in a power law multiplicative way. Toward establishing the precise form of (14), study through laboratory experiments of the effect of the sedimentological and hydrological characteristics (slope, input water and sediment discharge, and grain size) on the evolution and scaling exponents of braided rivers is needed, and this is an important issue for future research. Such studies will permit transferability of results from one system to another and from laboratory to nature.

8. Appendix: Scaling of the Number of Changes in a Fractal Object With the Size of the Observed Region

Here we will illustrate by example that the number of changes scales with the size of the observed region as written in (2). Consider, for example, a 3×3 Sierpinsky carpet with one square taken out (black area) such that every bigger square contains eight smaller ones and is a replication of the smaller squares at a larger scale (see Figure 7). The fractal dimension of this Sierpinsky carpet is $D = \log 8/\log 3$. Let us allow evolution of this carpet. The details of the evolution rules are not important for our purpose as long as the fractal dimension of the carpet is preserved. Similarly to what we did for braided rivers, we define changes in the evolving Sierpinsky carpet as parts of the space which were not occupied by the carpet at a certain moment of time but became occupied after some time lag. Since by definition the changes can only occur in the parts of the space occupied by the object (i.e., in the eight white squares), the cumulative number of changes in the 3 times larger square is 8 times the number of changes in a smaller square: $n_{\text{larger}}/n_{\text{smaller}} = (L_{\text{larger}}/L_{\text{smaller}})^D = 8$. In other words, the cumulative number of changes scales with the size of the observed region, with the scaling exponent equal to the fractal dimension of the generating fractal object. To avoid confusion, it should be noted that fractality of the spatial pattern of changes is not needed for the cumulative number of changes to scale as written in (2). For example, in the Sierpinsky carpet the cumulative number of islands (black parts) of a given size scales with the size of observation, with an exponent D (it increases $3^D = 8$ times when the scale is increased 3 times). However, the spatial pattern of the islands is not a fractal object at all (it has a nonzero Lebesgue measure).

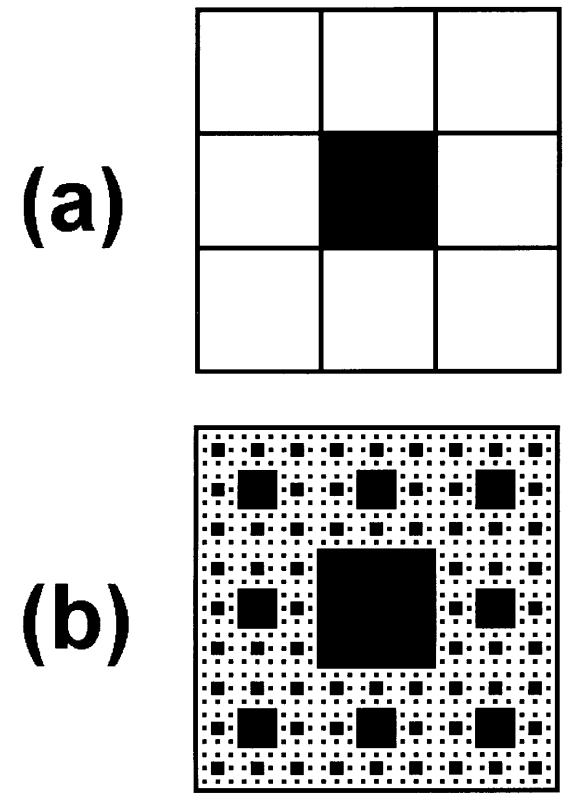

Figure 7. (a) The generator of a 3×3 Sierpinsky carpet with one square taken out (solid area) and (b) the Sierpinsky carpet.

Acknowledgments. This research was partially supported by NSF grant EAR-9628393. Supercomputer resources were kindly provided by the Minnesota Supercomputer Institute. We would like to thank Chris Paola, Gary Parker, and Alin Carsteanu for very helpful discussions, A. Brad Murray for tracing the image of the experimental braided river, and David Mohrig and Ben Erickson for help with the experimental equipment and setup. We would also like to thank the three anonymous reviewers for their helpful comments which resulted in an improved presentation of our developments.

References

Ashmore, P. E., Laboratory modelling of gravel braided stream morphology, *Earth Surf. Processes Landforms*, *7*, 201–225, 1982.

Ashmore, P. E., Process and form in gravel braided streams: Laboratory modelling and field observations, Ph. D. thesis, Univ. of Alberta, Edmonton, Alberta, Canada, 1985.

Ashmore, P. E., How do gravel-bed rivers braid?, *Can. J. Earth Sci*., *28*, 326–341, 1991.

Bak, P., and M. Paczuski, Why nature is complex, *Phys. World*, *12*, 39–43, 1993.

Bak, P., C. Tang, and K. Wiesenfeld, Self-organized criticality: An explanation of $1/f$ noise, *Phys. Rev. Lett*., *59*, 381–384, 1987.

Barzini, G. N., and R. C. Ball, Landscape evolution in flood—a mathematical model, *J. Phys. A Math Gen*., *26*, 6777–6787, 1993.

Czirok, A., E. Somfai, and T. Vicsek, Experimental evidence for self-affine roughening in a micromodel of geomorphological evolution, *Phys. Rev. Lett*., *71*, 2154–2157, 1993.

Edwards, S., and D. Wilkinson, The surface statistics of a granular aggregate, *Proc. R. Soc. London A*, *381*, 17–31, 1982.

Family, F., Scaling of rough surfaces: Effect of surface diffusion, *J. Phys. A Math Gen*., *19*, L441–L446, 1986.

Family, F., and T. Vicsek (Eds.), *Dynamics of Fractal Surfaces*, World Sci., River Edge, N. J., 1991.

Howard, A. E., and T. R. Knutson, Sufficient conditions for river meandering: A simulation approach, *Water Resour. Res*., *20*, 1659–1667, 1984.

Howard, A. D., M. E. Keetch, and C. L. Vincent, Topological and geometrical properties of braided streams, *Water Resour. Res*., *6*, 1674–1688, 1970.

Kadanoff, L. P., S. R. Nagel, L. Wu, and S. Zhou, Scaling and universality in avalanches, *Phys. Rev. A*, *39*, 6524–6537, 1989.

Kardar, M., G. Parisi, and Y. Zhang, Dynamic scaling of growing interfaces, *Phys. Rev. Lett*., *56*, 889–892, 1986.

Kuhnle, R. A., An experimental study of braiding in gravel-bed streams, M.S. thesis, Univ. of Illinois, Chicago, 1981.

Leddy, J. O., P. J. Ashworth, and J. L. Best, Mechanisms of anabranch avulsion within gravel-bed braided rivers: Observations from a scaled physical model, in *Braided Rivers*, edited by J. L. Best and C. S. Bristow, pp. 119–127, Geol. Soc. of London, London, England, 1993.

Ma, S. K., *Modern Theory of Critical Phenomena*, Benjamin, White Plains, N. Y., 1976.

Mandelbrot, B., *The Fractal Geometry of Nature*, 468 pp., W. H. Freeman, New York, 1982.

Meakin, P., P. Ramanlal, L. Sander, and R. Ball, Ballistic deposition on surfaces, *Phys. Rev. A*, *34*, 5091–5103, 1986.

Murray, A. B., and C. Paola, A cellular automata model of braided rivers, *Nature*, *371*, 54–57, 1994.

Parker, G., and E. D. Andrews, On the time development of meander bends, *J. Fluid Mech*., *162*, 139–156, 1986.

Patashinskii, A. Z., and V. L. Pokrovskii, *Fluctuation Theory of Phase Transitions*, 321 pp., Pergamon, Tarrytown, N. Y., 1979.

Rinaldo, A., I. Rodriguez-Iturbe, R. Rigon, E. Ijjasz-Vasquez, and R. L. Bras, Self-organized fractal river networks, *Phys. Rev. Lett*., *70*, 822–825, 1993.

Sapozhnikov, V. B., and E. Foufoula-Georgiou, Study of self-similar and self-affine objects using logarithmic correlation integral, *J. Phys. A Math Gen*., *28*, 559–571, 1995.

Sapozhnikov, V. B., and E. Foufoula-Georgiou, Self-affinity in braided rivers, *Water Resour. Res*., *32*, 1429–1439, 1996a.

Sapozhnikov, V. B., and E. Foufoula-Georgiou, Do the current landscape evolution models show self-organized criticality?, *Water Resour. Res*., *32*, 1109–1112, 1996b.

Schumm, S. A., and H. R. Khan, Experimental study of channel patterns, *Geol. Soc. Am. Bull*., *83*, 1755–1770, 1972.

Schumm, S. A., M. P. Mosley, and W. E. Weaver, *Experimental Fluvial Geomorphology*, chap. 1, pp. 1–7, Wiley-Interscience, New York, 1987.

Smith, L. C., B. L. Isacks, R. R. Forster, A. L. Bloom, and I. Preuss, Estimation of discharge from braided glacial rivers using ERS 1 synthetic aperture radar: First results, *Water Resour. Res*., *31*, 1325–1329, 1995.

Smith, L. C., B. L. Isacks, A. L. Bloom, and A. B. Murray, Estimation of discharge from three braided rivers using synthetic aperture radar satellite imagery: Potential application to ungaged basins, *Water Resour. Res*., *32*, 2031–2034, 1996.

Stølum, H. H., River meandering as a self-organization process, *Nature*, *271*, 1710–1713, 1996.

Takayasu, H., and H. Inaoka, New type of self-organized criticality in a model of erosion, *Phys. Rev. Lett*., *68*, 966–969, 1992.

Tang, C., and P. Bak, Critical exponents and scaling relations for self-organized critical phenomena, *Phys. Rev. Lett*., *60*, 2347–2350, 1988.

Vicsek, T., *Fractal Growth Phenomena*, World Sci., River Edge, N. J., 1992.

E. Foufoula-Georgiou and V. B. Sapozhnikov, Saint Anthony Falls Laboratory, University of Minnesota, Mississippi River and 3rd Avenue SE, Minneapolis, MN 55414. (e-mail: efi@mykonos.safhl.umn.edu)

(Received October 31, 1996; revised February 2, 1997; accepted April 23, 1997.)